E3S Web of Conferences **728**, 01002 (2026) https://doi.org/10.1051/e3sconf/202672801002
EEUPD 2026

Dynamic Coupling of Topographic Stability and Socio-Economic Exposure in Flood Risk Mapping: A Decadal Analysis of Honghu Dong Flood Detention Basin, Yangtze River (2014–2024)

Han Wang, Jiaming Liu*, Chengwei Lu

Changjiang Institute of Survey, Planning, Design and Research Co., LTD, Key Laboratory of Water Grid Project and Regulation of Ministry of Water Resources, Wuhan, China

Abstract: Dynamic flood risk mapping is crucial for adaptive management of Flood Detention and Retention Areas. This study proposes a novel "topography-socioeconomics-risk" dynamic coupling framework to quantify flood risk evolution in the Honghu Dong Flood Detention Basin (2014–2024), integrating MIKE FLOOD-based hydrodynamic modeling and Geographic Information System-driven spatial analysis. Multi-source data (LiDAR topography, socio-economic statistics) revealed: (1) Negligible topographic changes (<0.01 m elevation shift) maintained stable inundation patterns under the 1954 flood scenario; (2) Rapid socio-economic transitions increased population by 11.1% (28.6 thousand people) and GDP by 123.3% (from 4 to 9 billion CNY), while cultivated land shrunk 42.8% (203 km²), intensifying exposure of high-value assets; (3) Economic losses surged from 2.96 to 4.94 billion CNY, with commercial losses contributing 39.1% (782 million CNY) to the increment. The framework uniquely deciphers synergies between geomorphic stability and socio-economic dynamics, demonstrating that urbanization-driven asset concentration dominates risk escalation, rather than terrain changes. This paradigm provides a actionable tool for optimizing flood storage strategies in rapidly developing basins, prioritizing adaptive policies for high-value zones.

1. Introduction

Flooding is a highly destructive natural disaster in China that can cause enormous economic loss and human fatalities in basin areas [1]. In 2024, floods in China resulted in direct financial losses of 263.04 billion CNY and affected 534 million people, as reported by the Office of the National Committee for Disaster Prevention, Mitigation, and Relief. As a pivotal component of China's river basin flood control system, flood detention and retention areas mitigate flood risks by strategically impounding excess floodwaters and attenuating peak discharges, thereby safeguarding major downstream cities and critical flood-prone regions [2]. Accurate flood risk assessment in these areas is essential for operational safety and informed decision-making in flood control operations.

As a pivotal deliverable of flood risk assessment, flood risk maps provide spatially explicit visualization of inundation extents, water depths, and socio-economic impacts. Flood risk maps play an important role in integrated water resources management, such as land-use planning, engineering design optimization for flood control infrastructures, risk-informed emergency response planning, flood insurance implementation, and community risk perception enhancement. Flood risk mapping has stimulated extensive applied research domains, for instance, RAQUEL et al. conducted flood vulnerability assessment of international heritage building, flood risk map of Portuguese monuments was drawn through a comprehensive analysis of the geographical location and structure of the buildings, and strategies for the protection of cultural heritage were proposed [3]. TALEB et al. developed GIS-based flood risk maps for Mecca Province through a spatial analysis for the topography, rainfall pattern, drainage network density and sub-catchment areas, identifying urbanization pathways resilient to flash flood risks, the result shows that the drainage area and the density of the drainage network are the core two factors controlling the spatial differentiation of flash floods and should be given priority consideration in urban planning [4]. Addressing coastal flood risk mapping inaccuracies, ERIK et al. integrated public disaster registries (the Administration of the Republic of Slovenia for Civil Protection and Disaster Relief) to recalibrate the flood risk map for Piran, Slovenia, enhancing prediction reliability for historic urban preservation [5]. OGAREKPE et al. established watershed-scale flash flood risk maps by analyzing drainage system drivers, proposing targeted mitigation measures [6], while KLAUS et al. created national agricultural flood risk maps through an agricultural crop loss model, guiding for federal statewide coordinated designation of retention areas [7]. Although significant progress has been made in the construction and application of flood risk maps, several limitations persist. On one hand, the absence of dynamic coupling mechanisms: Existing studies predominantly focus on static topographic features or isolated socioeconomic

wanghan@cjwsjy.com.cn, *liujiaming@cjwsjy.com.cn, luchengwei@cjwsjy.com.cn (C.W.)

factors influencing flood risk, yet fail to quantitatively analyze the synergistic effects between topographic stability and socioeconomic dynamics. Particularly in rapidly urbanizing regions, the driving mechanisms of risk evolution arising from their interactions remain unclear. On the other hand, spatiotemporal limitations of data: Most risk maps rely on historical static data, which struggle to capture rapid changes in land use, population density, and economic activities during urbanization processes.

In 2013, the National Flood Control and Drought Relief Headquarters, in collaboration with the Ministry of Finance, officially initiated a nationwide project to compile flood risk maps for key areas, with particular emphasis on critical national flood detention and retention areas, assessing the flood risks associated with various flood storage schemes. The flood risk maps in flood detention and retention areas depict flood inundation details such as maximum inundation extent, inundation Depth, and flood impact information, which have significantly contributed to guiding regional flood control strategies, disaster reduction planning, and evacuation protocols. The Honghu Dong Flood Detention Basin is a strategic component of Hubei Province's "Two Circles and One Belt" development framework and a key flood control asset for the Yangtze River Basin, serving as a floodwater reservoir protecting the Jingjiang Levee and Wuhan City. The flood risk map of the Honghu Dong Flood Detention Basin, completed in 2015, which utilized topographic and socio-economic data of 2014, played an irreplaceable role in safeguarding the Yangtze Basin while fostering local socio-economic growth.

However, rapid socio-economic development and topographic changes within the Honghu Dong Flood Detention Basin have rendered existing risk maps insufficiently precise. This study addresses this gap by integrating multi-source heterogeneous socio-economic data and high-resolution topographic measurements (2014–2024) to develop a coupled 1D-2D hydrodynamic model using MIKE Flood software, and an impact analysis framework based on Geographic Information System (GIS). This work systematically evaluates topographic and socio-economic dynamics on flood risk evolution, delivering updated risk maps to enable precision flood management at the basin scale.

The remainder of this paper is organized as follows: The methodology is described in Section 2, including the overview of the Honghu Dong Flood Detention Basin, the data source, the flood analysis model, and the flood impact assessment method. The results and discussion are presented in Section 3, followed by the conclusions in Section 4.

2. Methodology

2.1 Study Area: Honghu Dong Flood Detention Basin

The Honghu Dong Flood Detention Basin (HDFDB) is geolocated at 113°24'E-114°24'E, 29°54'N-30°10'N, with elevation ranging from 16-33m. The HDFDB is situated in eastern Honghu city, Jingzhou prefecture, Hubei province, bordered by the Dongjing River to the north, the Yangtze River to the east and south, the Yaokou levee to the west, and is traversed by the Neijing River flowing west to east (shown in Figure 1). Administratively, it encompasses 6 towns (Wulin, Longkou, Yanwo, Xintan, Huangjiakou, Chahe), 1 township (Laowanxiang), and 2 county-controlled districts (Datong, Dasha), totaling 9 administrative units.

The HDFDB spans 873.70 km², with a designed impoundment water level of 30.47 m and an effective storage capacity of 6.47 billion m3. Hydraulic infrastructure includes the Taokou gate (inlet sluice, design inflow is 8,000 m3/s) and Buyuan gate (outlet sluice, design outflow is 2,000 m³/s), critical for flood regulation.

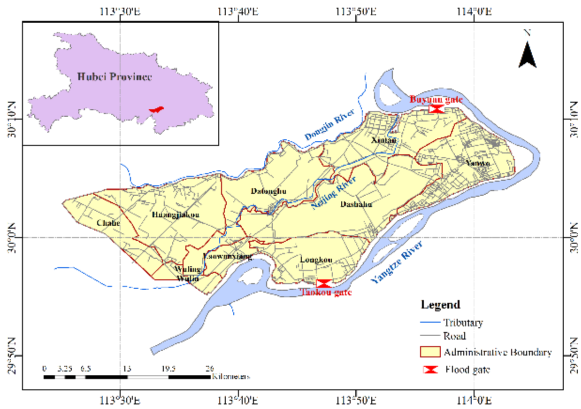

Fig. 1. Geographical Context of the Honghu Dong Flood Detention Basin, Middle Yangtze River.

2.2 Multi-Source Data Integration

The template is used to format your paper and style the text. All margins, column widths, line spaces, and text fonts are prescribed; please do not alter them. You may note peculiarities. For example, the head margin in this template measures proportionately more than is customary. This measurement and others are deliberate, using specifications that anticipate your paper as one part of the entire proceedings, and not as an independent document. Please do not revise any of the current designations.

2.2.1 Socio-economic Data

This study collected multi-source heterogeneous socio-economic datasets, including the database of resident property registration in HDFDB from 2005 to 2024, the Honghu Statistical Yearbook (1995 to 2024), and the Third National Land Survey dataset of China.

The annual resident property registration database of HDFDB is a statistical dataset of resident property in national flood detention and retention areas, organized by the National Flood Control and Drought Relief Headquarters and filled out by each province. The database mainly includes the population, cultivated land area, number of professional aquaculture, residential area, and agricultural production machinery of each administrative region in the flood detention and retention area. The statistical data on population, cultivated land area, and residential area were retrieved for administrative regions in the HDFDB for the target years 2014 and 2024.

The Honghu Statistical Yearbook is organized and compiled by the Honghu city government, which comprehensively integrates multi-source data such as censuses, sample surveys, administrative records, and big data. Processed through rigorous quality control protocols including cleansing, verification, and correction, these statistics accurately reflect yearly economic-social dynamics while maintaining exceptional data accuracy and credibility. GDP and three-sector industry output data were retrieved for administrative regions in the HDFDB for the target years 2014 and 2024.

China's Third National Land Survey dataset is an authoritative foundational repository comprehensively documenting territorial utilization patterns, initiated by the State Council and jointly executed by the Ministry of Natural Resources and National Bureau of Statistics, encompasses eight land categories, including croplands, woodlands, grasslands, wetlands, and built-up areas. This study utilized this dataset to determine the area and spatial distribution of industrial and commercial land in the HDFDB.

2.2.2 Topographic Data

The historical topographic dataset of 2014 is acquired from Hubei Provincial Department of Natural Resources, which is developed through integrated aerial photogrammetry, satellite remote sensing, and total station surveys, incorporating automated generalization with ArcGIS-standardized database workflows at a 1:10,000 scale for province-wide land coverage, meeting geospatial planning and resource management benchmarks.

The topographic dataset of 2024, captured via LiDAR-equipped drones over the HDFDB, was generated with 2 m-resolution DEMs via Delaunay TIN interpolation, with point cloud density exceeding 50 pts/m² validated by 235 ground control points.

Bathymetric data of the Yangtze River's main channel were compiled by the Changjiang Water Resources Commission at 1:10,000 mapping precision.

2.3 Flood Analysis Model

The pivotal phase in flood risk mapping involves conducting inundation analysis to identify flood parameters (spatial extent, water depth, etc.). Hydrodynamic modeling, recognized as a predominant approach for flood propagation simulation, has spawned multiple commercial software solutions, including MIKE Flood [8,9], SWMM [10], and Info Works-ICM [11]. The MIKE FLOOD flood simulation software, developed by DHI in Denmark, is employed to construct a flood analysis model. This model dynamically integrates the one-dimensional river module (MIKE 11) and the two-dimensional surface runoff module (MIKE 21), thereby providing a more realistic simulation of the flood routing situation in the HDFDB, rather than focusing solely on a single module.

2.3.1 River Network Hydraulics (MIKE 11)

The river flood simulation framework implemented in this study centered on a MIKE 11-based one-dimensional hydrodynamic model. The governing equations comprising both the continuity equation and momentum conservation principles are discretized through finite-difference approximation, with spatial-temporal differentiation achieved via the six-node Abbott-Ionescu scheme. Numerical resolution of the resultant algebraic system is executed through the catch-up algorithm, adhering to the methodological protocols established in [12].

The one-dimensional hydrodynamic model domain spans from Luoshan to Hankou, incorporating 1,622 river cross-sections with an average 2.5km spacing along the channel.

Given the catastrophic 1954 Yangtze floods (historically unprecedented in magnitude, duration, and peak stages across mid-lower reaches), this study adopts the 1954 flood as design flood, with Luoshan Station's recorded hydrograph defining upstream inflow and Hankou Station's stage-discharge relationship specifying downstream boundary.

2.3.2 Surface Inundation Simulation (MIKE 21)

The MIKE 21 model employs two-dimensional diffusive flow formulations with ADI second-order finite difference schemes to solve continuity and momentum equations, applicable to vertically homogeneous free-surface flows.

In this research, the MIKE 21 computational domain is discretized using unstructured triangular meshes with maximum edge lengths of 10m, generating 64,000 cells from 2014 and 2024 topographic datasets. Flood diversion operations in HDFDB are controlled through the Taokou gate, initiated at a base water level of 21.02m in the detention area.

2.3.3 Dynamic Coupling of 1D and 2D Modules (MIKE Flood)

The MIKE FLOOD platform implements dynamic coupling between the MIKE 11 and MIKE 21 hydrodynamic models. The coupled model itself does not carry out hydraulic calculations, but only through the coupling method, location, and related parameter settings, so that the one and two-dimensional models real-time exchange data, work together, flexible and stable calculations [8]. It has the strengths of one-dimensional and two-dimensional models, and at the same time, it can avoid the problem of lack of accuracy when a single model is used [13].

2.4 Flood Impact Assessment Method

Flood impact assessment primarily employs geospatial analytical methodologies to evaluate socioeconomic consequences. This approach systematically integrates inundation parameters (spatial extent and inundation depth) derived from hydrodynamic simulations with socioeconomic datasets from the HDFDB, enabling comprehensive flood risk evaluation.

2.4.1 Social impact analysis

The methodology initiates with the construction of three core databases: geospatial infrastructure, flood hydrodynamic characteristics, and vulnerability indicators. Standardized preprocessing protocols are implemented, including topological validation, coordinate system unification, and vertical datum normalization. Socioeconomic data undergoes spatial disaggregation through density weighting algorithms, with township-level demographic statistics being georeferenced to residential parcel features.

Utilizing the overlay analysis function of GIS software, inundation layers were integrated with administrative boundary layers, cultivated land layers, and residential area layers. This process yielded quantified data on submerged administrative regions, inundated cultivated land areas, and flooded residential zones under varying flood scenarios and inundation depth classifications.

Population exposure estimation utilizes township-level administrative units as fundamental analysis cells. Demographic spatialization techniques apply residential area-weighted density allocation, with population distribution coefficients derived from kernel density analysis. The affected population is subsequently calculated using the following formula:

$$P_e = \sum_i \sum_j A_{i,j} \times d_{i,j} \quad (1)$$

where Pe represents the affected population; Ai,j indicates the affected residential are of the jth residential plot in the ith administrative unit; di,j represents the population density of the jth residential plot in the ith administrative unit.

After determining the spatial distribution of the affected population, other related indicators such as affected GDP and residential area can be further deduced on this basis.

2.4.2 Economic Impact analysis

The economic impact of floods on flood detention and retention areas is jointly determined by danger, exposure, and vulnerability. This study adopts the method of constructing a loss rate model and combines GIS spatial analysis to calculate the economic impact [14]. This article divides the economic impact of flood detention and retention areas into the losses of five types of assets: family property, residence, agriculture, industry, and commerce. The calculation formulas for each type of loss are as follows:

$$S_i = \sum Q_i \times D_{iL} \times A_{iL} \quad (2)$$

where S_i represents the loss of the i-type asset; Q_i represents the unit value of i-type asset; D_{iL} is the loss rate of i-type asset under the Lth inundation level; A_{iL} is the inundation area of i-type asset under the Lth inundation level.

The determination of the value of various assets: For the asset values of agriculture, industry, and commerce, the data from the statistical yearbooks of each year are selected. For family properties, the replacement cost method is adopted. Combined with the relevant data of Honghu city, the replacement cost of residential buildings is 59.97 million yuan per square kilometer, and the per capita household assets amount to CNY 25,000. The economic loss rates are derived from the 2015 flood risk mapping project for the HDFDB, as shown in Table 1.

Table 1. Loss Rate Sensitivity to Inundation Depth in Honghu Dong Flood Detention Basin.

Inundation Level	Inundation Depth (m)	Family property (%)	Residence (%)	Agriculture (%)	Industry (%)	Commerce (%)
1	0.05-0.5	3	18	3	3	4
2	0.5-1.0	15	24	15	15	16
3	1.0-1.5	22	37	18	18	20
4	1.5-2.0	29	45	22	22	25
5	2.0-2.5	34	54	26	26	29
6	2.5-3.0	42	64	29	29	34
7	>3	50	80	80	32	38

3. Results and Discussion

3.1 Socioeconomic Transitions and Exposure Escalation

Table 2 presents the changes in key socio-economic indicators for each administrative region within the HDFDB from 2014 to 2024. As shown in the table, during the period from 2014 to 2024, there has been an increase in both population (11.1%) and residential area (2.9%) within the HDFDB, quantitatively translating to a net increase of 2,800 individuals, alongside a 0.3 km2 expansion in residential area. Conversely, the cultivated land area in the HDFDB has notably decreased by 42.8%, with a reduction of nearly 203 km2 over a decade. Meanwhile, the regional GDP has experienced substantial growth, increasing from 4 billion CNY in 2014 to approximately 9 billion CNY in 2024, representing a growth rate exceeding 120%. To further validate the statistical significance of the observed population and GDP growth trends, we applied the Mann-Kendall trend test. The results indicate that both growth trends during the period 2014-2024 are statistically significant at the $P < 0.05$ level, confirming that the observed changes (11.1% population growth and 123.2% GDP growth) are not attributable to random fluctuations. This significant economic progress can primarily be attributed to the development of water transportation along the Neijing River, which has facilitated the transformation of industries in coastal administrative regions. For instance, Huangjiakou has transitioned from traditional agriculture to specialized agriculture, while Xintan, Datonghu, and Dashahu have achieved rapid industrial and commercial development.

The social and economic changes in different administrative regions within HDFDB vary, which is due to differences in development policies, geographical locations, etc. Yanwo has always been dominated by agriculture and has gradually expanded its cultivated land area. In 2024, it has one quarter of the cultivated land area within the district, accounting for 15% of the GDP. Xintan is adjacent to the Neijing River, Dongjing River, and the Yangtze River, enjoying a favorable geographical location. It is a concentrated area of industrial parks within the flood detention area and has always been an economic center (with a GDP share of over 35%).

Socioeconomic trajectories across administrative units within the HDFDB exhibit marked disparities, attributable to divergent development policies and geographical determinism. Yanwo, historically entrenched in agricultural production, demonstrates progressive cropland expansion; by 2024, it contains one-quarter of the basin's cultivated land while contributing 15% to regional GDP. Conversely, Xintan's strategic positioning along the Neijing River, Dongjing River, and Yangtze River confluence confers locational advantages, hosting the detention basin's primary concentration of industrial parks and consistently maintaining its status as the economic nucleus (GDP contribution exceeding 35%).

Table 2. Socio-Economic Transition in Honghu Dong Flood Detention Basin (2014–2024): Population, Land Use, and GDP Dynamics.

Area	Population (people)			Cultivated land area (km^2)			Residential area (km^2)			GDP (hundred million)		
	2014	2024	Rate of change (%)	2014	2024	Rate of change (%)	2014	2024	Rate of change (%)	2014	2024	Rate of change (%)
Wulin	1266	9113	619.8	2	7.3	288.9	0	0.1	166.7	0.1	2.2	2080
Yanwo	38488	40975	6.5	56	72.7	29.6	1.7	1.8	2.3	3.2	14.1	335.3
Longkou	48991	51356	4.8	70	41.3	-41.3	1.9	1.7	-13.4	4	10.1	151.7
Huangjiakou	35818	37856	5.7	73.3	36	-50.6	1.3	1.8	35.6	4.2	6.1	45
Laowanxiang	15059	15373	2.1	17.3	13.3	-23.6	0.8	0.5	-34.7	1	2.3	136.4
Xintan	38409	39451	2.7	46	48	5.1	2.1	1.9	-8.2	17.7	34.8	97
Dashahu	36154	38410	6.2	101.3	22	-78.2	1.5	1.6	6.8	5.8	10.7	83.6
Datonghu	35292	37580	6.5	94	12	-87.3	2	2	3.6	3.3	5	51.8
Chahe	8646	16589	91.9	16.7	20	19.3	0.3	0.6	110.7	1	4.6	383.2
Whole area	258123	286703	11.1	475.3	272	-42.8	11.6	11.9	2.9	40.3	89.9	123.2

3.2 Geomorphic Stability and Its Implications

Figures 2 and 3 present topographic maps of the HDFDB for 2014 and 2024, respectively, with Table 3 quantifying administrative unit-specific mean elevation values. Geospatial analysis reveals a characteristic basin geomorphology characterized by a central topographic depression encircled by marginally elevated peripheries. Decadal comparative assessment of hypsometric distributions (2014 vs 2024 DEMs) coupled with administrative unit elevation statistics demonstrates remarkable geomorphic stability (The elevation change is less than 0.01m), suggesting anthropogenic terrain modifications remain statistically negligible.

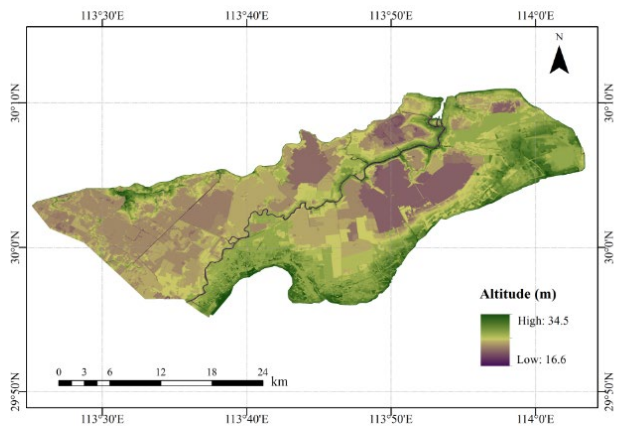

Fig. 2. Topographic map of the Honghu Dong Flood Detention Basin in 2014.

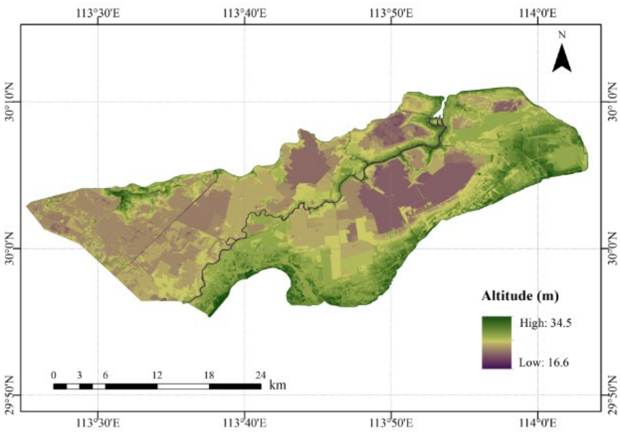

Fig. 3. Topographic map of the Honghu Dong Flood Detention Basin in 2024.

Table 3. Average elevation in the Honghu Dong Flood Detention Basin (2014 vs. 2024).

Area	2014 (m)	2024 (m)
Whole area	23.07	23.07
Wulin	23.59	23.58
Yanwo	24.36	24.35
Longkou	24.25	24.25
Huangjiakou	22.53	22.54
Laowanxiang	24.49	24.48
Xintan	23.13	23.13
Dashahu	22.47	22.47
Datonghu	22.62	22.62
Chahe	22.38	22.38

3.3 Flood Risk Dynamics

3.3.1 Inundation Patterns under Geomorphic Stability.

Based on the terrain of the Honghu Dong Flood Detention Basin, a GIS-based storage capacity calculation tool was used to compute the actual water levels corresponding to different flood volumes. The results were compared and validated against the average water levels simulated by the flood routing model. As shown in Table 4, the comparison indicates that the error in the simulated water levels from the flood routing model is within 0.05 m, demonstrating the model's reliability and suitability for subsequent research.

Table 4. Validation of Simulated Water Levels from the 2D Model for the HonghuDong Flood Detention Area

Discharge (100 million m^3)	Simulated water level (m)	Actual Water Level (m)	Error (m)
5	25.59	25.54	0.05
10	26.16	26.12	0.04
15	26.73	26.70	0.03
20	27.3	27.27	0.03
25	27.87	27.85	0.02
30	28.44	28.43	0.01
35	29.01	29.00	0.01
40	29.58	29.58	0.00
45	30.15	30.16	-0.01
50	30.72	30.74	-0.02
55	31.29	31.31	-0.02

Figures 4 and 5 depict the 1954 flood inundation depths in the HDFDB under the 2014 and 2015 terrain conditions, respectively, while Table 5 presents the average inundation depths across administrative regions within the basin. Due to minimal inter-annual terrain variations in the HDFDB, the flood inundation patterns under different topographic scenarios remain nearly identical. Following the 1954 flood diversion event, the entire basin experienced complete submergence, with a mean inundation depth of 7.43 meters. Within the HDFDB, Chahe exhibits the lowest average elevation and the deepest flooding (8.12 m), contrasting with Laowan, which has the highest elevation and shallowest inundation (6.02 m).

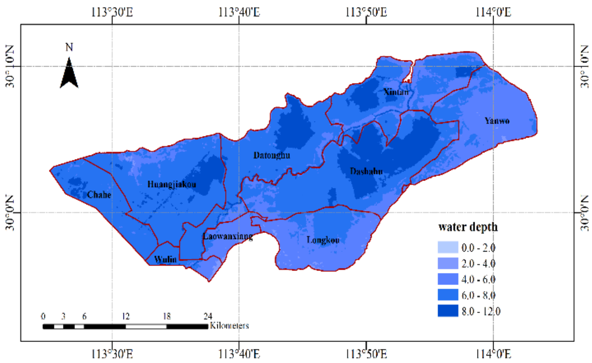

Fig. 4. The flood inundation depth map of the Honghu Dong Flood Detention Basin in 2014.

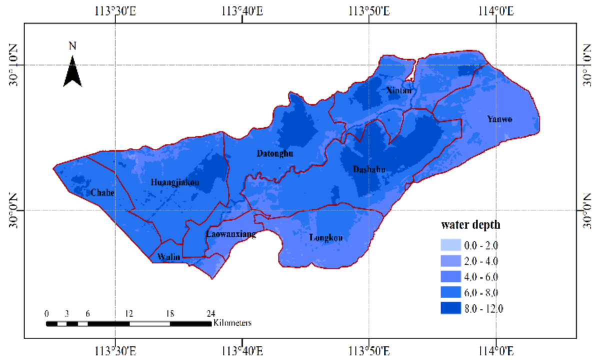

Fig. 5. The flood inundation depth map of the Honghu Dong Flood Detention Basin in 2024.

Table 5. Average inundation depth n the Honghu Dong Flood Detention Basin (2014 vs. 2024).

Area	2014 (m)	2024 (m)
Whole area	7.43	7.43
Wulin	6.91	6.92
Yanwo	6.14	6.15
Longkou	6.25	6.25
Huangjiakou	7.97	7.96
Laowanxiang	6.01	6.02
Xintan	7.37	7.37
Dashahu	8.03	8.03
Datonghu	7.88	7.88
Chahe	8.12	8.12

3.3.2 Population Exposure and Residential Vulnerability

Table 6 shows the statistics of the social impact of flood inundation in the segmented flood detention and storage areas of Honghu East. Theoretically, the changes in the social impact of flood inundation in flood detention areas are influenced by topography and socio-economic changes. Given that the topography changes in the flood detention area from 2014 to 2024 are extremely minor, the changes in the social impact of floods from 2014 to 2024 are consistent with the changes in socio-economic factors within the area. When the Honghu East Block flood detention area is used for flood diversion, the affected population and housing increase slightly, the area of inundated cultivated land decreases, and GDP is the most affected, increasing from 4.026 billion yuan to 8.985 billion yuan.

Table 6 presents the statistical data on flood inundation-induced social impacts in the HDFDB. Theoretically, variations in these social impacts are driven by both topographic dynamics and socioeconomic shifts. However, due to negligible topographic changes observed in the detention area between 2014 and 2024, the evolution of flood-related social impacts during this period aligns solely with socioeconomic transformations within the region. Upon activation of the HDFDB diversion, the affected population and residential areas exhibited a marginal increase, whereas the area of affected cultivated land decreased. Notably, GDP experienced the most pronounced impact, rising from CNY 4.02 billion to CNY 8.98 billion.

Table 6. Social impact of Honghu Dong Flood Detention Basin from 2014 to 2024.

Year	Affected population (thousand people)	The area of affected cultivated land (km^2)	The area of affected residence (km^2)	Affected GDP (hundred million)
2014	258.1	475.3	11.55	40.26
2024	286.7	272.0	11.88	89.85

3.3.3. Commercial Asset Sensitivity and Loss Escalation

Table 7 summarizes the economic impacts of flooding in the HDFDB. Under the 2014 topographic and socioeconomic conditions, the total economic loss during the 1954 flood storage event amounted to CNY 295,900, predominantly attributed to agricultural losses (CNY 143,100). Under the 2024 topographic and socioeconomic conditions, flood diversion in the HDFDB would result in total economic losses of CNY 4.94 billion, primarily comprising agricultural losses (CNY 1.914 billion) and commercial losses (CNY 1.416 billion). With socioeconomic development, total flood losses in this compartment have increased by nearly CNY 2 billion, of which commercial losses experienced the fastest growth, rising from CNY 634 million to CNY 1.416 billion.

Based on the research findings, strategic adjustments to the current flood risk management system are recommended. First, shift protection priorities from traditional sectors like agriculture and residences to commercial districts and the tertiary industry. Second, introduce innovative financial instruments by developing differentiated commercial flood insurance products with risk-based pricing, leveraging market mechanisms to disperse risk. Third, enhance business resilience by guiding enterprises in business continuity planning and optimizing post-disaster compensation and credit support policies. These measures will facilitate rapid business recovery, safeguarding local economic vitality and employment stability.

Table 7. Economic Loss of Honghu Dong Flood Detention Basin from 2014 to 2024 (100 millions CNY).

Year	Family property loss	Residential loss	Agricultural loss	Industrial loss	Commercial loss	Total economic loss
2014	2.76	4.26	14.31	1.90	6.34	29.59
2024	6.15	5.69	19.14	4.25	14.16	49.40

4. Conclusions

This study focuses on the Honghu Dong Flood Detention Basin, with 2014 and 2024 as comparative baseline years. Socioeconomic datasets and high-resolution topographic data were integrated to develop a MIKE-based 1D-2D coupled hydrodynamic model, augmented by GIS-driven flood impact assessment frameworks. A decade-long analysis (2014–2024) reveals:

(1) From 2014 to 2024, the terrain change in the HDFDB is very minor, with the elevation change being less than 0.01m, indicating that human activities within the HDFDB have a weak effect on terrain modification.

(2) From 2014 to 2024, there is a slight increase in the population and residential area in the HDFDB, increasing by 11.1% (28,600 people) and 2.9% (0.3 square kilometers), respectively. The area of cultivated land has decreased significantly, by 42.8% (nearly 203 square kilometers). The GDP grew rapidly, increasing from CNY 4 billion in 2014 to CNY 9 billion.

(3) Given the minor topographic changes in the HDFDB, the flood inundation characteristics in 2024 are almost the same as those in 2014. When the 1954 flood is used for flood diversion, all areas within the HDFDB are submerged, with an average inundation depth of 7.43 meters.

(4) Given the significant changes in the social economy of the HDFDB, when the area was diverted by the 1954 flood, the total economic loss in 2024 increased by nearly CNY 2 billion compared with that in 2014. Among them, the commercial loss increases the most significantly, by nearly CNY 800 million.

While the empirical findings of this study are geographically constrained to a specific flood storage compartment, the developed analytical framework for assessing spatiotemporal flood risk dynamics demonstrates universal methodological applicability. This research advances systemic comprehension of risk evolution mechanisms in managed floodplains while establishing a data-driven foundation for adaptive flood diversion policy formulation. Methodologically, the adoption of constant asset valuation metrics across temporal scenarios (due to limited historical pricing data) introduced quantifiable uncertainties in loss estimation accuracy. Future investigations should prioritize multi-source socioeconomic data acquisition, particularly time-variant property valuation datasets, to enable temporally granular impact assessments.

Acknowledgment

Funding: This research was funded by the National Key Research and Development Program project (2024YFC3012302), the National Key Research and Development Program project (2023YFC3209102), the National Natural Science Foundation of China (Grant No. 52079037), Major Science and Technology Project of the Ministry of Water Resources (Grant No. SKS-2022003), Scientific Research Project of Changjiang Institute of Survey, Planning, Design and Research Co., Ltd(Grant No.CX2024z04-2).

References

1. Gao, L.; Liu, X.; Liu, H. Spatiotemporal differentiation characteristics of flood risk based on spatial statistical analysis: a study of Jing–Jin–Ji

region in China. Natural Hazards. 2024, 121(2), 1-26. DOI: 10.1007/s11069-024-06876-8.

2. Wang, H.; Liu, J.M.; Tan, Z.Y.; et al. Dynamic risk assessment of flood detention basins based on flood diversion volume control: A case study of the Honghu East Block. Journal of Yangtze River Scientific Research Institute, 2025, 1-9. https://link.cnki.net/urlid/42.1171.tv.20250828.1440.006.
3. Raquel, B.; Ana S.G.; Joao M.P.Q.; Delgado. Rising damp in Portuguese cultural heritage - a flood risk map. Structural survey, 2016,34, 43-56. DOI: 10.1108/SS-07-2015-0034
4. Taleb, O.; Abbas, I.; Alakhras; Mohamed, H.; et al. A Recommended Urban Plan According to Flash Flood Risk Potential Map: The Case Study of Mecca Province - Saudi Arabia. International journal of sustainable development and planning: Encouraging the unified approach to achieve sustainability, 2022, 17,737-742. DOI:10.18280/ijsdp.170304.
5. Erik, K.; Peter, K.; CÉCIL, J.W.; Meulenberg. Coastal Flood Risk Assessment: An Approach to Accurately Map Flooding through National Registry-Reported Events. Journal of Marine Science and Engineering, 2023,11. https://www.mdpi.com/2077-1312/11/12/2310
6. Ogarekpe.; Nkpa, M.; Nnaji; Chidozie, C.; Ekpenyong; Maurice G. Flash Flood Risk Assessment of the Great Kwa River Basin Using Analytical Hierarchy Process. Water Conservation Science and Engineering, 2022,7,599-611. DOI:10.1007/s41101-022-00167-8.
7. Klaus; Stefan; Kreibich; Heidi; Merz, Bruno; et al. Large-scale, seasonal flood risk analysis for agricultural crops in Germany. Environmental earth sciences,2016,75. DOI: 10.1007/s12665-016-6096-1.
8. Yin, W.; Liu, J.; Feng, H.; et al.Study of flooding hazards in highly urbanized area based on a coupled one- and two-dimensional hydrological-hydrodynamic model. Desalination and Water Treatment, 2025. DOI: 10.1016/j.dwt.2024.100933
9. Pareta, K.; Pareta, U. A review of cloudbursts events in the Himalaya region, and 2D hydrodynamic simulation using MIKE models. Natural Hazards, 2025, 121(8), 1-33. DOI:10.1007/s11069-025-07173-8.
10. Li, J.; Feng, J.; Wang, Q.; et al. Construction-Induced Waterlogging Simulation in Pinglu Canal Using a Coupled SWMM-HEC-RAS Model: Implications for Inland Waterway Engineering. Water, 2025, 17(16), 2415. DOI:10.3390/W17162415.
11. Xue, R. Flood Simulation and Improvement Scheme Study of a Drainage System Based on the Infoworks ICM Model. China Flood & Drought Management, 2024, 34(S1), 28-31.
12. Ahmed, F. Numerical modeling of the Rideau Valley Watershed. Nat Hazards 2010; 55:63–84. DOI: 10.1007/s11069-010-9588-4.
13. Zandsalimi, Z.; Feizabadi, S.; Yazdi, J.; Neyshabouri, S. Evaluating the impact of digital elevation models on urban flood modeling: a comprehensive analysis of flood inundation, hazard mapping, and damage estimation. Water Resour Manag 2024, 38, 4243–68. DOI:10.1007/s11269-024-03862-4.
14. Li, L.; Shan, Y.Q.; Yang, J.Y. Impact Assessment of Flood Disaster on Industrial Economic System. China Flood & Drought Management, 2025, 1-11. https://doi.org/10.16867/j.issn.1673-9264.2025168.